Experimental and theoretical investigation of the electronic structure of silver deposited onto InSb(110) at 10 K

V. Yu. Aristov,* M. Bertolo,† K. Jacobi, F. Maca,‡ and M. Scheffler
Fritz-Haber-Institut der Max-Planck-Gesellschaft, Faradayweg 4-6, D-1000 Berlin 33, Germany
(Received 23 November 1992; revised manuscript received 3 May 1993)

Ag films of thickness z with $0.5 \leq z \leq 60$ monolayers (ML) evaporated onto a cleaved InSb(110) substrate at 10 K have been investigated through angle-resolved uv photoelectron spectroscopy (ARUPS) using synchrotron radiation and low-energy electron diffraction (LEED). The band structure has been calculated for bcc and fcc Ag. Inclusion of spin-orbit interaction makes the band structure near Γ very similar for bcc and fcc structures, whereas in the outer part of the Brillouin zone towards L and N distinct differences exist. From comparison between calculations and measurements we find some evidence that at 10 K and using an InSb(110) substrate bcc Ag is formed for thicknesses $2.5 \leq z \leq 30$ ML. The LEED pattern also indicates that bcc Ag is formed with Ag(110)||InSb(110) as it was recently observed by Aristov *et al.* Annealing films with $z > 5$ ML to 300 K transforms these bcc films into fcc (111)-oriented Ag clusters. A 60-ML-thick annealed film exhibits as perfect ARUP spectra of the 4*d* bands as measured for a Ag(111) single-crystal surface, but exhibits no LEED pattern. For the thin bcc films a quantum-well state is observed.

I. INTRODUCTION

The preparation of thin metal films under ultrahigh-vacuum (UHV) conditions is a growing field in solid-state physics. The conditions created during UHV deposition of thin metal films can be quite different from conditions in nature. Therefore, one expects even new crystalline phases which can help to better understand solid-state physics. The investigation of structure and properties of thin metal films on semiconductor substrates is also important for the development of new microelectronic devices. In the future the density of elements of integrated circuits will reach such a high degree that all electronic processes will take place within few atomic layers between interfaces. It is therefore very important to study the changes an interface imposes onto the properties of thin films.

A number of metastable phases as a result of deposition of thin noble- and transition-metal films onto different substrates have been observed recently, e.g., body-centered cubic (bcc): Cu,[1–4] Ni,[5,6] Co,[7] and Cr;[5] face-centered cubic (fcc): Fe;[8–11] body-centered tetragonal (bct): Cu,[12] Mn,[13] Fe.[14] In theoretical articles[15–17] the possibility for the existence of such phases has also been confirmed.

In a previous low-energy electron diffraction (LEED) and Auger electron spectroscopy (AES) study of Ag deposition on InSb (110) at 10 K and for film thicknesses z with $2.2 \leq z \leq 10$ monolayers (ML's) a new Ag phase was observed.[18] The LEED pattern corresponds to a (110) plane of the bcc structure which is unusual for Ag: at ambient pressure Ag is fcc up to its melting point. The evaluation of the unit cell was very reliable, because keeping the substrate surface, in part, free of deposited atoms it was possible to observe two diffraction patterns, from the clean substrate and from the Ag film, simultaneously. The following relationships between the film and the substrate are valid: $(110)\mathrm{Ag}_{\mathrm{bcc}} \| (110)\mathrm{InSb}$; $[1\bar{1}0]\mathrm{Ag}_{\mathrm{bcc}} \| [1\bar{1}0]\mathrm{InSb}$; $[001]\mathrm{Ag}_{\mathrm{bcc}} \| [001]\mathrm{InSb}$. From these LEED observations the lattice constant for three-dimensional (3D) bcc Ag was derived as $a_{\mathrm{bcc}} = 3.35$ Å. In all other publications mentioned above,[1–14] for the ordered adlayer the same LEED or reflection high-energy electron diffraction pattern was observed as for the substrate. The main argument for the existence of unusual film structures mostly used in these contributions was the interlayer spacing normal to the surface as obtained from LEED spectra. On the other hand, in Ref. 18, although bcc-Ag(110)||InSb(110) and the analogous crystallographic directions in a (110) plane of either structures (film and substrate) are coincident, two diffraction patterns could be simultaneously observed indicating that the Ag adlayer is aligned but not in registry with the InSb substrate.

The question of bcc versus fcc structure of Ag has been recently addressed by Maca and co-workers[19,20] through total-energy and electronic-structure calculations. At zero temperature and pressure the bcc structure has only slightly higher energy. However, for negative pressure the total energy is smaller for bcc than for fcc. If the volume per atom reaches 15% more than that of the equilibrium volume of the fcc structure, the bcc structure would become favorable. The corresponding lattice constant should be ≈ 3.37 Å which agrees with the experimental observation for Ag films at InSb(110).[18] However, it is important to recognize that the bcc and fcc structures are two special cases of the general tetragonal lattice—the bcc structure may be viewed as a continuous distortion of the fcc, and vice versa. The large variety of tetragonal variations have not yet been examined for obvious practical reasons. One could constrain the Ag lattice parameter in plane via deposition onto an

appropriate substrate to match that predicted for bcc Ag, but there is no reason to expect a true bcc structure to result, as a tetragonal configuration may come out at the total-energy minimum for that choice of in-plane spacings. This can also be the case for the deposition growth of Ag on InSb(110).

For the experimental results presented here, we will show that it is very difficult to separate bcc features at coverages below 10 ML from the fcc ones dominating for the thicker films. Therefore, it was important to reproduce the fcc band structure[21] in more detail in the calculations. The inclusion of spin-orbit (SO) interaction was necessary for this purpose. It is interesting to see that the bcc and fcc band structures become more similar by including SO interaction. Besides the comparison of the band structure along ΓL (for fcc) and ΓN (for bcc), symmetry considerations are of importance in discussing the experimental results.

In this paper we present an experimental and theoretical investigation of the evolution of the electronic structure of thin Ag films with a thickness up to 60 ML deposited onto InSb(110). It will be shown that, in accordance with the LEED pattern, there is some evidence that the electronic structure is bcc-like for annealed films up to 5 ML and for not annealed films up to 30 ML, whereas annealed films are fcc-like from about 10 ML on.

II. EXPERIMENTAL PROCEDURE

Photoemission mesaurements with synchrotron radiation were performed at the TGM 3 (toroidal grating monochromator) beam line of the Berlin Electron Storage Ring BESSY (Berliner Elektronenspeicherring-Gesellschaft für Synchrotronstrahlung). Angle-resolved UV photoelectron spectra (ARUPS) of the valence band were taken with a hemispherical electron energy analyzer (ADES 400, VG Scientific Ltd). Typically, a total instrumental resolution was achieved of better than 150 meV up to 60-eV photon energy. The measurements were performed with a bias voltage of -2.0 eV at the sample, which increases the kinetic energy of the photoelectrons by 2.0 eV. All spectra were recorded at normal emission. The angle of incidence of the light α, taken with respect to the surface normal, was varied between 15° and 75°. The azimuth of the incident light was varied through preparation of different samples. The light was polarized in the plane of incidence with the E vector nearly parallel to the surface for $\alpha=15°$ and nearly perpendicular for $\alpha=75°$.

Clean InSb(110) surfaces were obtained by cleavage *in situ* at 300 K. Samples with dopant concentrations of $n\approx 5\times 10^{16}$ cm^3 (tellur) were used. Only high-quality cleavages were investigated in our experiments. Ag was evaporated from a pre-outgassed tantalum wire heated by electric current. The coverages were measured by the time of deposition. The deposition rate was calibrated by Auger electron spectroscopy (AES). For the Ag film thickness calibration we used the Auger signal amplitudes of In (404 eV) and Sb (454 eV) obtained under identical conditions at $T\approx 10$ and 300 K using a quartz-oscillator thickness monitor placed near the sample surface in an earlier experiment.[18] A relative error in estimating the coverage by such a method amounts to $\approx 20-30\%$. The film thickness is given in units of ML [one ML corresponds to the number of Ag atoms equal to the number of atoms in the outer atomic plane of the fcc Ag(111) surface]. The deposition rate was varied within 0.25–0.75 ML/min. The total pressure of residual gases in the experiments was less than 7×10^{-11} Torr under deposition, otherwise 5×10^{-11} Torr at 300 K and below 3×10^{-11} Torr at 10 K.

The thin Ag films in the range between 2.6 and 60 ML were obtained by Ag deposition onto clean cleaved InSb (110) substrates cooled down to ≈ 10 K. The diffraction patterns were observed by a four-grid LEED optics. The ARUP spectra of Ag films were recorded at ≈ 10 K either immediately after deposition or after heating the samples to temperature ≈ 225 or ≈ 300 K. Any time after Ag deposition with film thickness z in the range $2.6\le z\le 60$ ML we have observed the same LEED pattern that was published in Ref. 18. We have found that the best pattern can be obtained in the coverage range between 2.5 and 8 ML. In the range $8\le z\le 60$ the sharpness and relative intensity of the diffraction spots deteriorate. Heating to 300 K and cooling down to 10 K again improved the diffraction pattern (diffraction spots were becoming stronger and sharper, and the background was significantly reduced) at all coverages studied. Results for the Schottky barrier formation during film growth have been published elsewhere.[22]

III. MODEL CALCULATIONS

Results of total-energy and band-structure calculations of fcc and bcc Ag, using the self-consistent, scalar-relativistic, linear muffin-tin orbitals (LMTO's) method, have recently been published by Said *et al.*[19] In calculating the density of states and photoemission spectra for fcc and bcc Ag, Maca, Kambe, and Scheffler[20] have used the non-self-consistent layer-Kohn-Korringa-Rostoker (LKKR) scheme and the muffin-tin potential of Moruzzi, Janak, and Williams.[22] For fcc Ag the lattice constant was taken from Moruzzi, Janak, and Williams.[23] ($a_{\rm fcc}=4.12$ Å). The bcc lattice constant $a_{\rm bcc}=3.37$ Å has been constructed from the geometry of the InSb substrate.[18] For both structures, touching muffin-tin spheres with the same diameter have been taken. Semi-infinite crystals are composed of identical planar layers parallel to the surface. The fcc (111) and bcc (110) surfaces are the two most closely packed surfaces of the fcc and bcc structures, respectively. In the fcc (111) surface (symmetry C_{3v}) the local geometry can be characterized by a parameter $d_1=a_{\rm fcc}/\sqrt{2}=2.91$ Å—the nearest-neighbor distance in the layer—and the interlayer spacing $d=2.38$ Å. To build the bcc (110) plane the symmetry of the local atomic configuration has to be changed into C_{2v}, four nearest neighbors in the plane stay in the distance d_1, and two others move to a distance $d_2=3.36$ Å. The interlayer distance is lowered to $d=2.36$ Å.

For this model the silver structure in the direction ΓL (for fcc) and ΓN (for bcc) have been calculated and are published elsewhere.[19,20] In the fcc crystal, localized d

states along Λ in the Brillouin zone (BZ) are split into two twofold Λ_3 bands and one single Λ_1 band and hybridize with free-electron-like *sp* states. There is no degeneracy of energy bands in the bcc structure. The bcc bands have symmetry Σ_1, Σ_2, Σ_3, and Σ_4.

In order to calculate an Ag fcc band structure which is in better agreement with the latest, widely used calculations[21] and measurements[24] we performed scalar-relativistic band-structure calculations. Figure 1 shows the calculated scalar-relativistic silver band structure in the ΓL (fcc) and ΓN (bcc) directions, without (left) and with (right) spin-orbit interaction. The tight-binding (LMTO) (Ref. 25) scheme has been used with potential parameters obtained from a scalar-relativistic self-consistent LMTO calculation for fcc silver.[26] The SO interaction influences more the fcc than the bcc bands by splitting the Λ_3 bands into Λ_6 and $\Lambda_{4,5}$ bands while the Λ_1 band is changed into Λ_6. All bcc bands hybridize together because they belong to Σ_5, the only representation of the group.

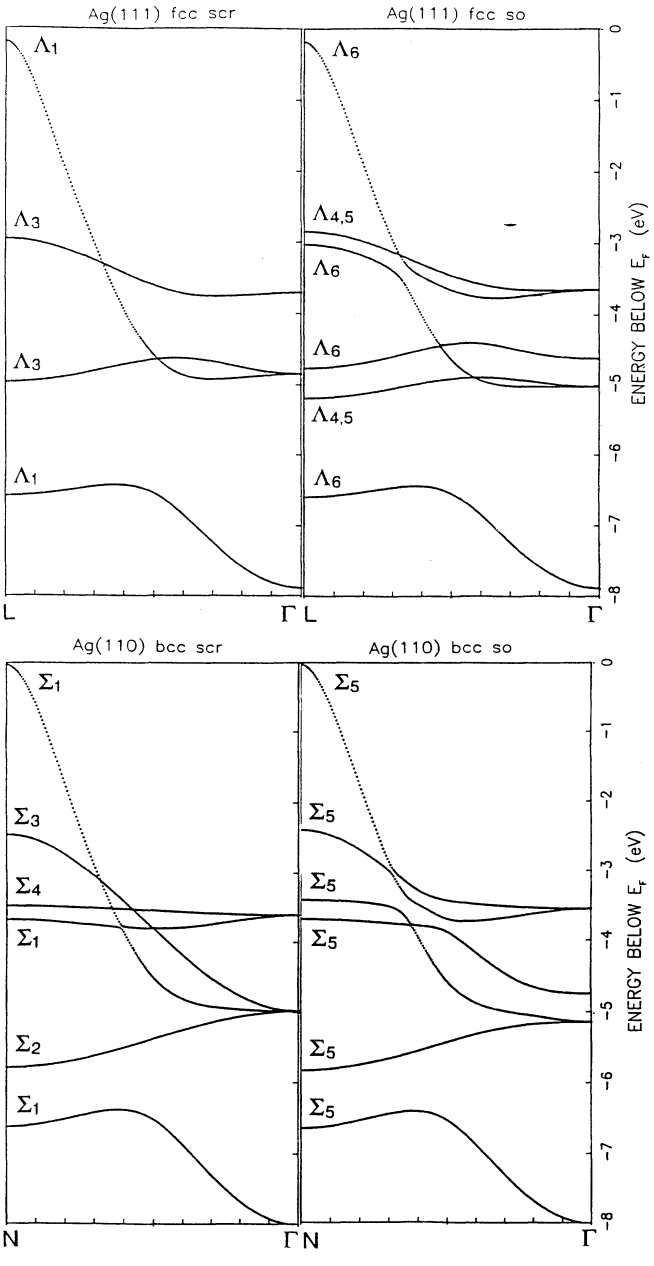

FIG. 1. Linearized muffin-tin orbital scalar-relativistic valence-band structure of fcc Ag along the ΓL direction (above) and for bcc Ag along the ΓN direction (below). The LMTO bands are calculated without (left panels) and with (right panels) spin-orbit interaction.

Close to Γ the energies as well as the shape of the valence bands of both structures are very similar. However, noticeable differences exist at the Brillouin-zone edge (see Fig. 1, right panel): There are two flat *d* bands at -4.8 eV and at -5.2 eV at the fcc *L* point, but no bands exist in this energy range at the bcc *N* point. Thus, transitions starting from such energy bands can be used to distinguish both structures.

In the following, we briefly discuss the dipole selection rules with respect to our ARUP spectra taken in normal emission. It is well known that direct photoemission transitions are governed by dipole selection rules. In the normal photoemission the final states have to be totally symmetric. For the photoemission from bcc (110) surfaces only initial states of symmetry Σ_1 and Σ_4 (Σ_1 and Σ_3) for the light source in the [001] ([110]) direction are allowed for *p*-polarized light. No such strong restriction exists for normal emission from fcc (111) surfaces (for *p*-polarized light initial states of symmetry Λ_1 as well as Λ_3 are possible). Therefore, the polarization-dependent photoemission experiments should provide strongest tests of energy band calculations along symmetry lines and they should distinguish both structures.

The nonrelativistic theory practically predicts identical normal emission spectra taken from the fcc (111) surface under two different azimuth angles of incident light ($\Phi=0°$ direction $[0\bar{1}1]$ and $\Phi=90°$ direction $[\bar{2}11]$). As mentioned above, in both cases the *p*-polarized light excites transitions from Λ_1 and Λ_3 valence bands. fcc (111) layers are highly symmetric and represent a compact atom ordering. In contrast, photoelectron spectra for *p*-polarized light at normal emission taken from a bcc (110) surface should manifest a strong orientation dependence. There are contributions to normal photoemission spectra starting from initial bands of symmetry Σ_3 ($\Phi\approx 0°$ direction [001]) or Σ_4 ($\Phi=90°$ direction $[1\bar{1}0]$).

We can take advantage of selection rule effects by comparing normal photoemission spectra taken under different polar angles α of the incident light.[27,28] For small α the component of the electric field parallel to the surface is large. With increasing α the transition excited by the component of the electric field parallel to the surface will be gradually suppressed. Such a dependence is predicted for *p*-polarized spectra taken from both silver modifications—to the transitions from bands of symmetry Λ_1 (Σ_1) α-dependent contributions starting from bands of symmetry Λ_3 (Σ_3 or Σ_4) are expected.

The most important part of relativistic corrections is the spin-orbit interaction. It splits degenerated energy bands and hybridizes bands of originally different symmetry. Due to the lowering of the symmetry, there are

fewer selection rules. The effect of SO coupling is most drastic for the bcc(110) surfaces where now all initial states belong to Σ_5, the *only* representation of the double group (compare Fig. 1).

IV. EXPERIMENTAL RESULTS AND DISCUSSION

The presentation of our experimental results is divided into four subsections: IV A, thick Ag films; IV B, thin Ag films; IV C, preparation and dependence on thickness; and IV D, quantum-well states and film structure.

A. Thick Ag films

Our first example is a 60-ML Ag film, annealed to 300 K which is our best approximation of bulk Ag. Figure 2 exhibits a group plot of typical ARUP spectra for photon energies of 10 eV $\leq h\nu \leq$ 25 eV. In order to map the initial state, we have used the nearly free totally symmetric band which runs up to 16 eV above E_F from L to Γ taken from our LKKR band-structure calculations (the lowest-lying conduction band). In this energy range the Λ_1 band for fcc Ag is identical to the equivalent Σ_1 band calculated for bcc Ag. We use this band for all band mapping calculations. This is reasonable even near the gap at Γ (16 eV above E_F) since our ARUPS results indicate that this gap is closed in photoemission to a large extent. Nevertheless, we have used it only beyond the gap since our first goal is to differentiate fcc from bcc and not to perform a most complete band mapping.

Figure 3 exhibits the result of our simple calculation. We have connected the data points through smooth lines to guide the eye. The lines are drawn similarly to the calculation of Eckardt, Fritsche, and Noffke[21] for fcc Ag which reproduce the measured values of Wern *et al.*[24] very well. The lines are also in agreement with the calculated bands of Fig. 1; only the gap between the two *d*-derived Λ_6 bands in the middle of the Brillouin zone is wider. The choice of the bands connecting our data points indicates already that the band structure along ΓL is very indicative for fcc Ag. This becomes even clearer through the comparison with our calculation for bcc Ag, as shown in Fig. 1. It should be noted here that the calculated *d* bands are 1.2 eV closer to E_F. The discrepancy reflects the well-known problem of the local-density approximation (used in our calculations) in identifying Kohn-Sham eigenvalues with excitation energies. For the comparison of our calculated and measured bands the *d* bands of the calculation have to be shifted down by 1.2 eV relative to E_F and also relative to the *sp* band. This shift moves the crossing of the *sp* band with *d* bands somewhat to the right. Such a correction can easily be done by hand. In doing so, we can see that the fcc bands fit very well with all measured data whereas for the bcc bands large deviations are observed: (1) The overall width of the *d* band is larger for bcc Ag by 0.2 eV at Γ and by 0.5 eV at L (N). (2) The two flatbands in the second half of the BZ (near L) $\Lambda_{4,5}$ and Λ_6 around -5 eV in the calculation, i.e., -6 eV in the measurements, are clearly observed in the experiments and contradict the bcc band structure. (3) There is evidence in the experiments for the two upper Λ_6 and $\Lambda_{4,5}$ bands near L for which there is no counterpart in the bcc calculations. There is a weak feature, marked (1) in Fig. 3, which does not fit to the bcc bands and for which we did not find an

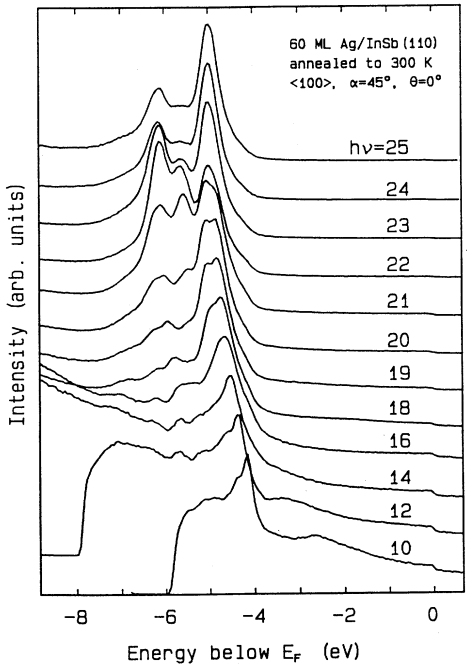

FIG. 2. Angle-resolved photoelectron spectra for an Ag film, 60 ML thick and annealed to 300 K. Azimuthal and polar angle α of the incident light of energy $h\nu$ are given. The spectra are measured at normal electron emission ($\theta = 0°$).

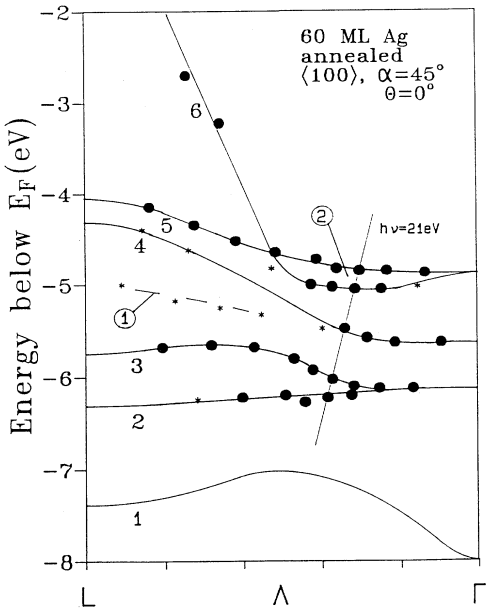

FIG. 3. Band structure of fcc Ag along ΓL. Dots and stars are the measured positions for a 60-ML-thick film. The lines are drawn to guide the eye through the points in accordance with calculations (Ref. 21). For further details see the text and the caption of Fig. 2.

explanation.

Our spectra are, in fact, better resolved than those in the most comprehensive measurements of Wern *et al.*[24] In the region marked (2) in Fig. 3 we have clearly resolved bands 5 and 6 for which one can see separated peaks in Fig. 2. This is also true for bands 2 and 3 when approaching Γ. In Fig. 3 we have connected the points measured at $h\nu=21$ eV where clearly five *d* bands are resolved. We observed the same variation in intensity of the different bands, found and discussed by Wern *et al.*[24] Bands 5 and 6 go through an intensity minimum near $h\nu=21$ eV, whereas bands 4, 2, and 3 reach maxima near $h\nu=23$ eV. This behavior was explained by Wern *et al.* due to the final-state gap between bands 7 and 8 near Γ.

Finally, we note that the *L*-gap surface state near E_F is not observed under our conditions. We believe that this observation is in accordance with the morphology of our Ag deposit which differs from that of the clean ordered crystal surface: There is no good long-range order achieved parallel to the surface; no Ag(111) LEED pattern is visible. We presume that 3D clusters have been formed with the (111) plane oriented parallel to the substrate and ordered surfaces smaller in size than found at the surface of single-crystallline Ag(111). This conclusion is also supported by the Auger data[18] and photoemission core-level data.[22]

Having established that for a 60-ML film an fcc Ag band structure has developed, exhibiting nearly every detail found for well-prepared Ag(111) single-crystal surfaces, we have asked how these findings change with decreasing film thickness. In Figs. 4 and 5 we show our results for an annealed 30-ML-thick Ag film. One recognizes that the main features are still observable. There is the *sp* part of band 6 around −3 eV. Bands 5 and 6 are not resolved. We have added data for band 1 which could not be so clearly separated from the background for the 60-ML film. In Fig. 5 we have drawn the same curves as in Fig. 3 which also connect quite reasonably the data points in this case. Therefore, we conclude that this film is still fcc-like.

In Fig. 6 we show the band structure for an 8-ML Ag film. The data are clearly compatible with the bands derived from the 60-ML film. It is evident that the *sp* part of the band structure is no longer seen. Instead, there are only three bands left, the two lower ones are practically dispersionless. This structure is still in good agreement with the calculation for fcc Ag(111) in Fig. 1 with SO interaction included and having the *sp* band (Λ_6) removed. The dispersion of the upper band indicates that the film is still a 3D solid-state object.

In summary, we have observed strong variations of the electronic structure between 60 and 8 ML. These films have in common that they belong to the class of fcc-ordered *d* metals. This observation changes if we go to even thinner films or change the preparation procedure, as it is discussed in the next section.

B. Thin Ag films

Figures 7 and 8 exhibit ARUP spectra for a 2.6-ML Ag film for *z*-polarized light, i.e., polarized mostly normal

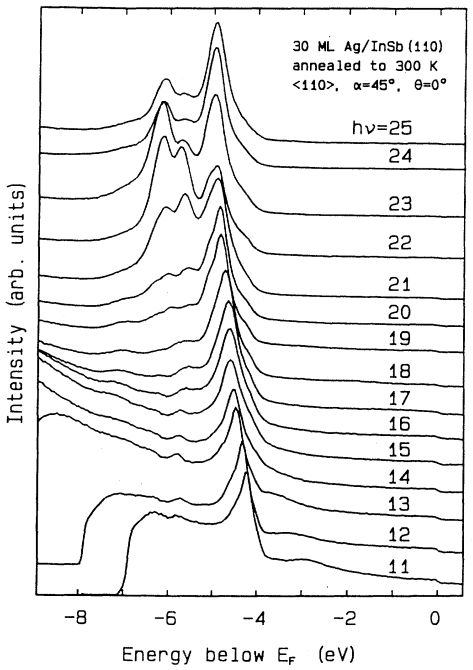

FIG. 4. ARUP spectra for a 30-ML fcc Ag film, annealed to 300 K. Azimuthal and polar angle α of the incident light of energy $h\nu$ are given. The spectra are measured at normal electron emission ($\theta=0°$).

to the surface ($\alpha=75°$, Fig. 7) and *x*-polarized light, i.e., polarized parallel to the surface and in the plane of incidence ($\alpha=15°$, Fig. 8). The Ag *d* band has developed to a width indicative of 3D interactions. This is supported

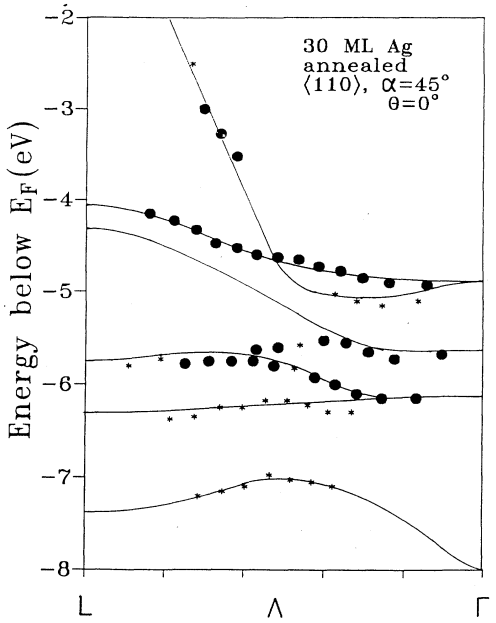

FIG. 5. Band structure of fcc Ag along Γ*L*. Dots and stars are the measured positions for a 30-ML-thick film. The lines are drawn to guide the eye through the points in accordance with known calculations (Ref. 21). For further details see the text and the caption of Fig. 2.

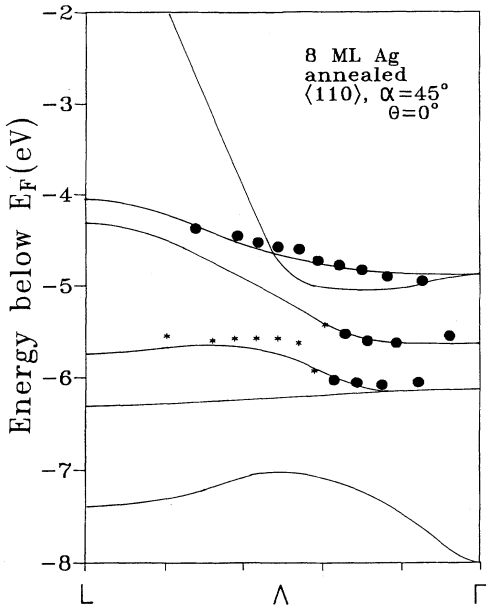

FIG. 6. Band structure of fcc Ag along ΓL. Dots and stars are the measured positions for an 8-ML-thick film. The lines are drawn to guide the eye through the points in accordance with known calculations (Ref. 21). For further details see the text and the caption of Fig. 2.

by comparison with the band structure for an ordered Ag ML at Al (111) (Ref. 29) which exhibits a smaller overall width. Furthermore, the peaks of Figs. 7 and 8 are rather pronounced, indicating a relatively good order of the

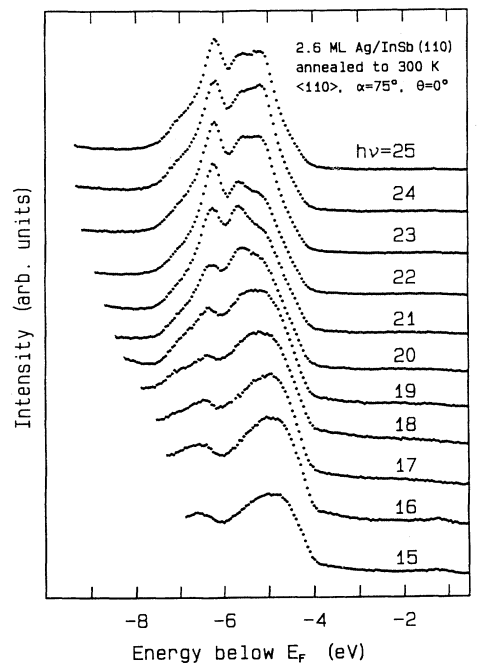

FIG. 7. Angle-resolved photoelectron spectra for an Ag film, 2.6-ML thick and annealed to 300 K. Azimuthal and polar angle α of the incident light of energy $h\nu$ are given. The spectra are measured at normal electron emission ($\theta=0°$).

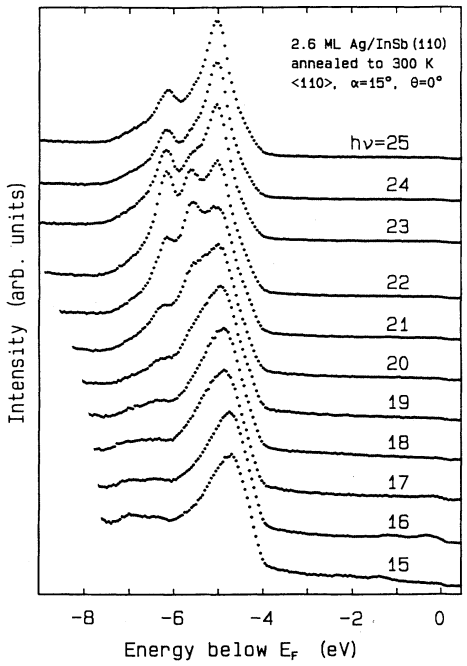

FIG. 8. Angle-resolved photoelectron spectra for an Ag film, 2.6-ML thick and annealed to 300 K. Azimuthal and polar angle α of the incident light of energy $h\nu$ are given. The spectra are measured at normal electron emission ($\theta=0°$).

film. This agrees with the observation of the typical LEED pattern for Ag/InSb(110).[18] The band structure along ΓN, determined for two films and the two polarization directions of light, is shown in Fig. 9. There is some scattering of the data points which one may expect for such thin films. Three main bands can be recognized at about -5, -5.5, and -6.3 eV (one should follow the full dots for this purpose). There is no indication of the *sp* band, as expected from the discussion of the 8-ML film above. We will discuss this point later.

Our interpretation of this band structure is the following: We can clearly decide that it is not an fcc structure. In order to see this better, one should compare the data with Fig. 6. The overall width of the bands is slightly larger, the center of gravity is shifted away from E_F, and, most important, there is a pronounced band [marked by (1) in Fig. 9] extending to $\frac{3}{4}$ of ΓN and exhibiting a much stronger intensity, as seen from the spectra in Figs. 7 and 8, than expected for an equivalent fcc film. Since we observe the same LEED pattern as found by Aristov, Bolotin, and Grazhulis[18] which has been assigned to the (110) plane of bcc Ag, we expect an Ag phase different to fcc. We believe that the electronic structure seen in our experiment supports the assignment of the LEED pattern, i.e., the thin Ag film is ordered according to *bcc Ag*. In order to make our assignment better understood we have included Fig. 10 in which we present the *d* bands for bcc (ΓN) and fcc (ΓL) Ag. The bands are derived from our calculations, as shown in Fig. 1, by shifting the bands downwards by 1.2 eV and removing the *sp* band. By overlaying Figs. 10 and 9, one recognizes that the bcc bands describe the trends in Fig. 9 better than the fcc

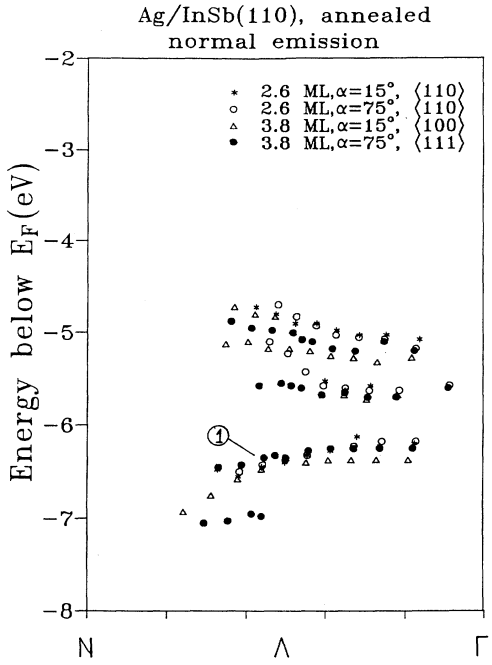

FIG. 9. Measured peak positions for thin annealed Ag films of different thickness as indicated along the ΓN or ΓL direction. Azimuthal and polar angle α of the incident light are given. For mark (1) see the text.

bands: (1) the bcc bands are shifted more downward; (2) their overall width is larger; (3) there is one band more in the upper half, i.e., three bcc bands are more spread out in energy than the two narrow-spaced fcc bands; and (4) the lower bands are much lower in energy and exhibit more dispersion. Point (3) can clearly be recognized in Figs. 8 and 9: away from Γ, in the middle of the BZ (i.e., for photon energies of 15 to 20 eV in Figs. 7 and 8) there is a broad overlapping emission centered at -5 eV. Point (4) is evident by comparing Figs. 9 and 6 as mentioned above.

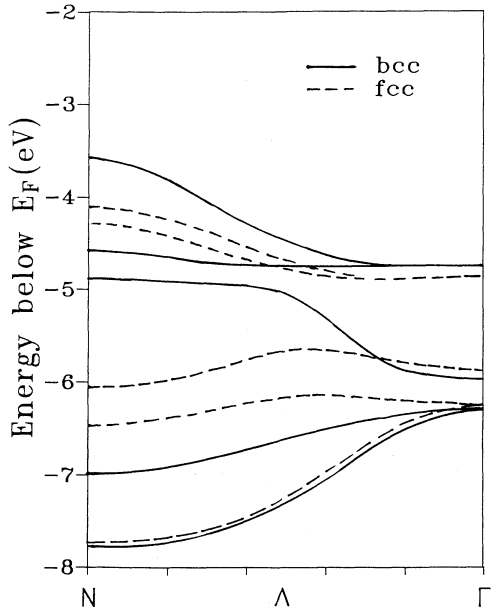

FIG. 10. Sketch of the band structure for bcc Ag (full lines, ΓN, Σ) and fcc Ag (broken lines, ΓL, Λ) according to the calculation of Fig. 1 after removal of the *sp* band and an appropriate shift with respect to E_F (see text).

Our assignment is also supported by the polarization dependence of the spectra. We argue here that we find a reminder of the dipole selection rules. Considering our calculations as shown in Fig. 1 without SO interaction, we find that for bcc (fcc) z polarization of light ($\alpha=75°$, Fig. 7) allows emission out of the Σ_1 (Λ_1) bands, whereas x polarization ($\alpha=15°$, Fig. 8) allows emission out of the Σ_4 (Λ_3) bands. This consideration supports that the upper bands of symmetry Λ_3 can be observed for fcc and only one band of symmetry Σ_4 (centered at -4 eV in the calculation, i.e., at -5 eV in the experiments) can be observed for bcc. The latter is the case as it is found by comparing Figs. 7 and 8. We get back to this point below.

So far we have discussed thin films which have been annealed. This thickness range was chosen since for thicknesses of slightly more than 2 ML an order-disorder transition is observed. For these thin films we have clear evidence that they are not ordered according to fcc, and we found that they are compatible with a bcc lattice, but with the band structure not being fully developed. For thicker films (≥ 8 ML) we have found a transformation into fcc. This observation is reasonable since a thicker Ag film of the bcc structure is expected to be strained so that it probably cannot withstand annealing up to 300 K. Therefore, we prepared a thick film of 30 ML but avoided annealing. Spectra for such a film are shown in Figs. 11 and 12. Surprisingly, most of the spectra exhibit very

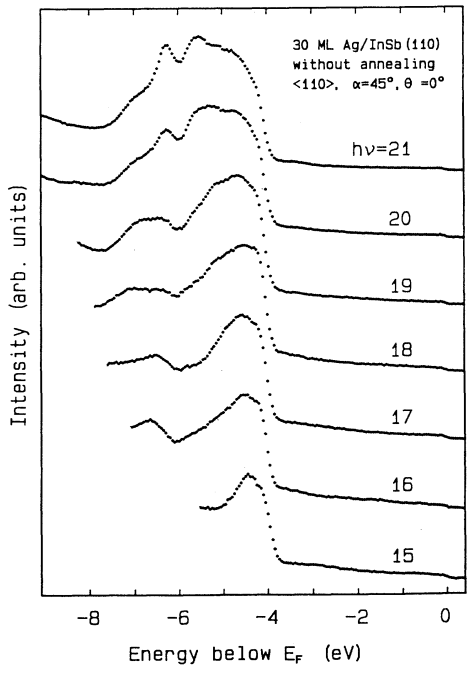

FIG. 11. Angle-resolved photoelectron spectra for an Ag film, 30 ML thick and without annealing. Azimuthal and polar angle α of the incident light of energy $h\nu$ are given. The spectra are measured at normal electron emission ($\theta=0°$).

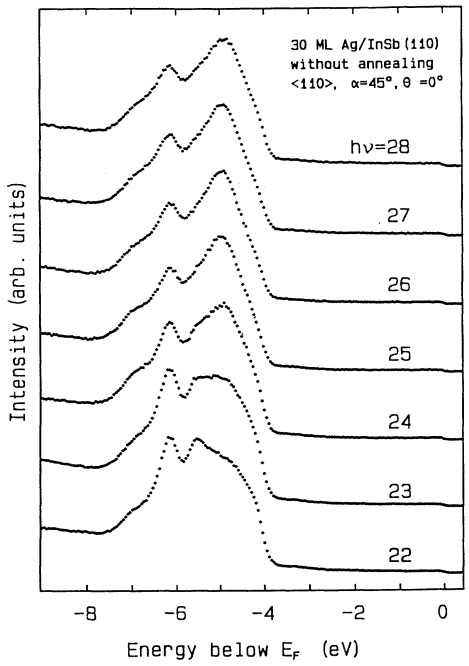

FIG. 12. Angle-resolved photoelectron spectra for an Ag film, 30 ML thick and without annealing. Azimuthal and polar angle α of the incident light of energy $h\nu$ are given. The spectra are measured at normal electron emission ($\theta=0°$).

sharp peaks, and the broad features are therefore likely to be due to overlapping bands. The result of band mapping is shown in Fig. 13. Together with the data points we have included lines which are the calculated bcc bands, including SO interaction from Fig. 1 with the d bands

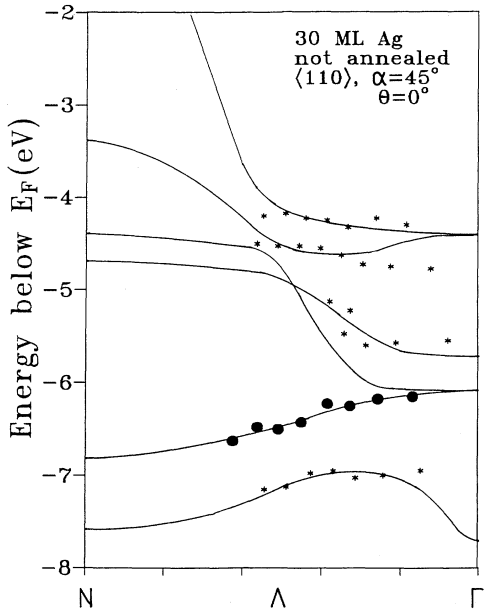

FIG. 13. Band structure of bcc Ag along ΓN. Dots and stars are the measured positions for strong and weak peaks for the 30-ML-thick film whose spectra are shown in Fig. 12. The lines are drawn by hand according to the calculation of Fig. 1 after shifting the Ag 4d with respect to the sp band (see text).

shifted by 0.9 eV away from E_F. There is a surprisingly good correlation between calculation and experiment. The comparison of the equivalent band structure for fcc Ag, which is shown in Fig. 5, indicates that there are differences. The result shown in Fig. 13 gives some evidence that we have been able to prepare Ag films of bcc structure thick enough so that the band structure is fully developed and thin enough so that they could withstand any anticipated strain. On the other hand, we have to admit that there are similarities between our spectra shown in Figs. 11 and 12 and polycrystalline fcc Ag films.[30] The fact that we did not have to anneal, in order to get ordered films, seems to be an inherent property of Ag which is known to become ordered at rather low temperatures. Additionally, it is known that photoemission is a rather local probe. Therefore, although the LEED pattern at 30 ML was not as good as for thinner films, the ARUPS results are still indicative for a bcc structure. From this insight one could speculate about an even better compromise on film thickness for a future experiment.

C. Preparation and dependence on thickness

Since we now understand what is observed for the thick films as well as for the thin annealed films, we are able to discuss the changes observed during annealing of the films. We would also like to comment on the development of the electronic structure with thickness. Before we get to these points, we will show how we have measured surface sensitivity and that the substrate emission does not interfere with Ag 4d emission.

Figure 14 exhibits ARUP spectra before and after evaporation of 0.5 ML of Ag. The observed substrate peaks are extremely sharp as compared to measurements of other groups at 300 K.[31,32] We observe two peaks due to the

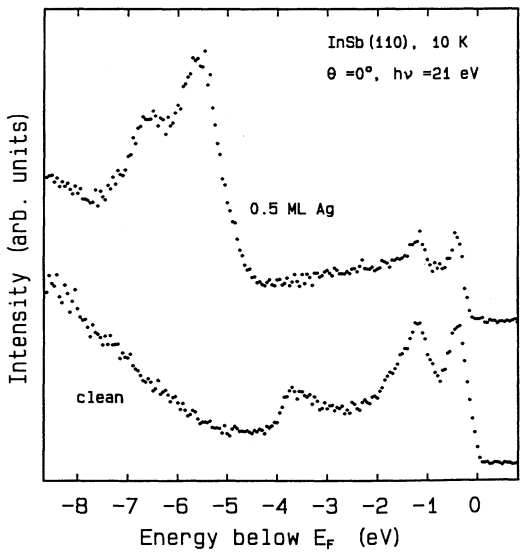

FIG. 14. ARUP spectra for the clean cleaved InSb(110) surface at 10 K and after deposition of 0.5-ML Ag at 10 K. Photon energy $h\nu=21$ eV. The spectra are measured at normal emission ($\theta=0°$).

bulk transitions at -0.15 and -1.00 eV below the valence-band maximum (VBM) and a surface resonance at -3.4 eV. We assume that our sample is slightly degenerate, i.e., E_F lies near the conduction-band minimum in the conduction band. Therefore, we have subtracted 0.2 eV to reference the peak position from Fig. 14 to the VBM (the band gap is 0.18 eV wide). We have not measured many spectra of the clean surface, since band mapping of InSb was not the goal of our work. From the weakening through the Ag adlayer we argue that the upper two peaks are from bulk transitions and the lower one is a surface resonance. Qualitatively, we know that at $h\nu=21$ eV we map the bands near the Γ point so that we expect up to three bands to be seen near the VBM. According to the calculations of Chelikowsky and Cohen[33] there is a split of 0.82 eV between the Γ_7 and Γ_8 states at the Γ point. This is in very good agreement with a split of 0.85 eV near Γ observed in our measurements. An In-derived surface resonance is expected at about 3 eV at the Γ point from calculations.[34] Since the peak at -3.4 eV is quenched completely after adsorption of half a ML of Ag, its character as a surface resonance is demonstrated. Interestingly, from our measurements of the core-level shifts during Ag adsorption,[22] we have concluded that at this coverage Ag is interacting with or being adsorbed near the In surface atoms. This explains the complete quenching of an In-derived surface resonance through adsorption of half a ML of Ag.

The spectra of Fig. 14 indicate that our measurements are from the so far best prepared surfaces (cleavage and cooled to 10 K). Furthermore, they visualize how strong the Ag 4*d* intensity is compared to the *sp* band intensity from the InSb substrate. Quite obviously the substrate emission is not interfering with the Ag emission. For more than 1 ML of Ag no individual InSb valence-band peaks are resolved, instead a broad emission is observed from InSb *sp* and Ag *s* states. At 2.5 ML a well-defined Fermi level is observed from which the energy zero point in Fig. 14 is deduced. The 4*d* signal in Fig. 14 (0.5 ML) is typical for single adsorbed atoms or 2D islands. For a film of 1.25 ML the base of the 4*d* emission is broadened by 0.8 eV and the peaks are shifted by 0.2 eV closer to E_F. This observation is also in agreement with our core-level measurements in which we came to the conclusion that single Ag atoms are adsorbed at coverages below 0.1 ML where they start growing together above 0.1 ML.

The next two figures confirm our assignment of bcc Ag. For the 1.6-ML Ag film in Fig. 15 the final value is reached for the base of the Ag emission. The spectra in Fig. 15 confirm that annealing of the thin films does not change the spectra very much. There is a change of spectra between 1.6 and 2.6 ML which we assign to a transition from disordered, amorphous to bcc Ag in accordance with the order-disorder transition observed in LEED. Figure 16 visualizes the changes in spectra with thickness. We have chosen a photon energy near the energy of the He I line used in the laboratory. Small but well-defined changes occur between 2.6 and 8 ML during the transition from bcc to fcc. The peak at 4.9 eV, indicative for the fcc phase, develops. It becomes stronger between 8 and 12 ML so that parts of the 8-ML film may

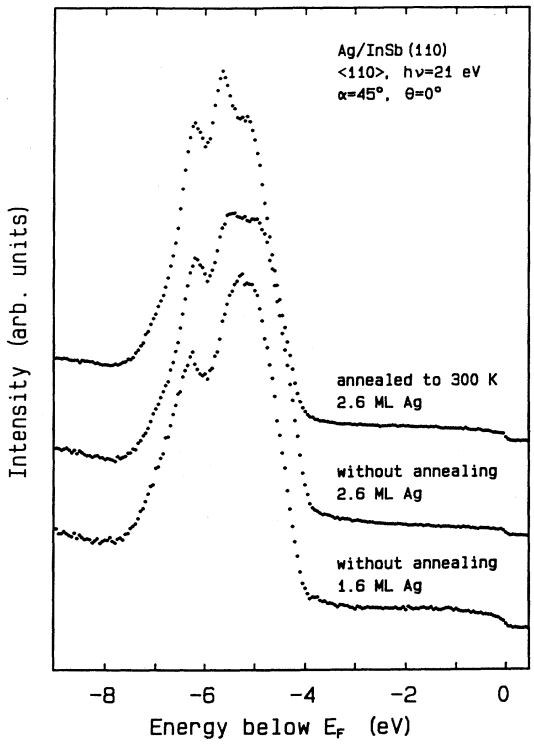

FIG. 15. ARUP spectra for differently prepared thin Ag films at the InSb(110) cleavage plane. Azimuthal and polar angle α of the incident light of energy $h\nu$ are given. The spectra are measured at normal electron emission ($\theta=0°$).

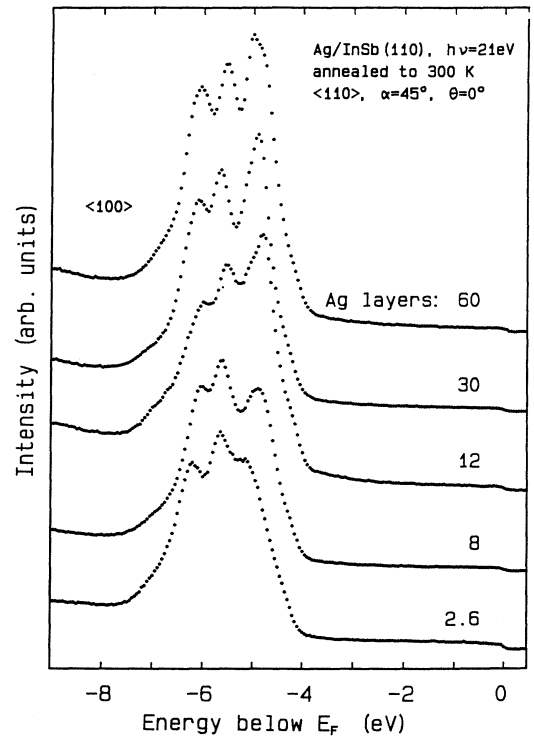

FIG. 16. ARUP spectra for Ag films of increasing thickness at a photon energy of $h\nu=21$ eV. Azimuthal and polar angle α of the incident light of energy $h\nu$ are given. The spectra are measured at normal electron emission ($\theta=0°$).

still be bcc-like. Between 12 and 30 ML the 4*d* emission becomes sharper, indicating more 3D interaction. For 60 ML (not shown, see Fig. 2) this sharpening continues so that, e.g., the upper peak is split into two. There is also a shift in energy for the peak near -6 eV by an amount of 0.2 eV between 2.6 and 8 ML.

D. Quantum-well states and film structure

Quantum-well states have been observed using ARUPS for a number of well-prepared thin metal films. An example is the Ag film on Cu(111) system studied by Mueller, Miller, and Chiang.[35] Although the misfit between Ag(111) and Cu(111) is large, Ag(111) grows very well ordered on Cu(111). The order is improved by annealing to 200 °C. At $h\nu=11$ eV a large number of quantum-well states is observed with an amplitude of up to 5% of the *L*-gap surface-state peak.

For our thin Ag films we also observed a quantum-well feature at about -1.8 eV below E_F which is a well-resolved peak for $h\nu=18$ eV as shown in Fig. 17. Between 14 and 16 eV there is a strong interference with the In 4*d* core-level emission due to second-order photons from the monochromator. The peak at -1.8 eV has all properties expected for a quantum-well state: It exhibits no dispersion with $k_\perp$, i.e., with variation of $h\nu$, as can be seen from Fig. 17. It disperses with θ, the angle of emission with respect to the surface normal, towards E_F. This reflects the dispersion of the initial-state *sp* band as discussed by Mueller, Miller, and Chiang.[35] We have noted earlier that the *sp* band in the energy range between E_F and -4 eV does not differ very much between fcc and bcc Ag so that we can compare our results for the bcc Ag film with those of Mueller, Miller, and Chiang[35] for fcc Ag. Furthermore, the peak at -1.8 eV becomes sharper by annealing the film to 300 K and its intensity increases for *z*-polarized light ($\alpha > 75°$).

For the thin bcc Ag films which exhibit the quantum-state peak, no *N*-gap surface-state (SS) emission can be observed. Taking into account the strong SS intensity for the Ag(111)/Cu(111) system one may conclude that the *N* gap does not reach beyond E_F. This contradicts our calculation. The answer to this question has to be left open since our database is not large enough for this special aspect.

For the thicker annealed films we do not observe any quantum-well state. Within the context of our other observations this is reasonable since we do not observe any SS intensity for the thicker annealed fcc Ag films either. A well-ordered film of uniform thickness is a prerequisite for the observation of quantum-well states since the energy of a quantum-well state depends on the thickness, and a thickness distribution means a superposition of quantum-well states of different energy, i.e., a smearing out of these features.

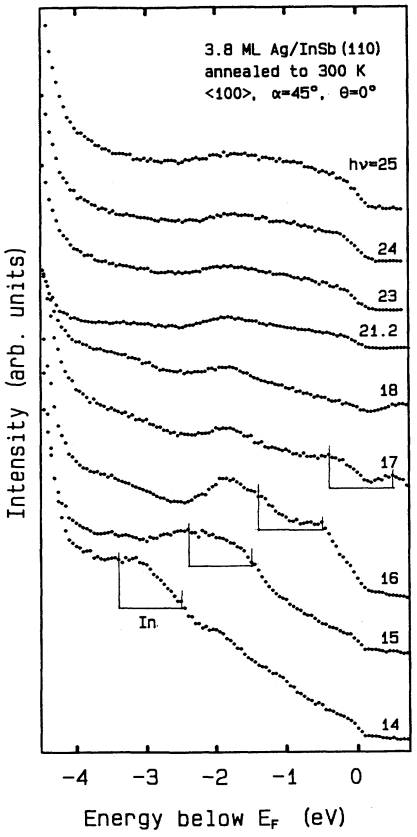

FIG. 17. ARUP spectra for the *sp* band region between E_F and the Ag 4*d* bands for a 3.8-ML-thick Ag film on InSb(110). The parameter is the photon energy $h\nu$. Azimuthal and polar angle α of the incident light of energy $h\nu$ are given. The spectra are measured at normal electron emission ($\theta=0°$).

V. OUTLOOK

From the discussion of our measurements it has become clear how difficult it is for the system Ag||InSb(110)

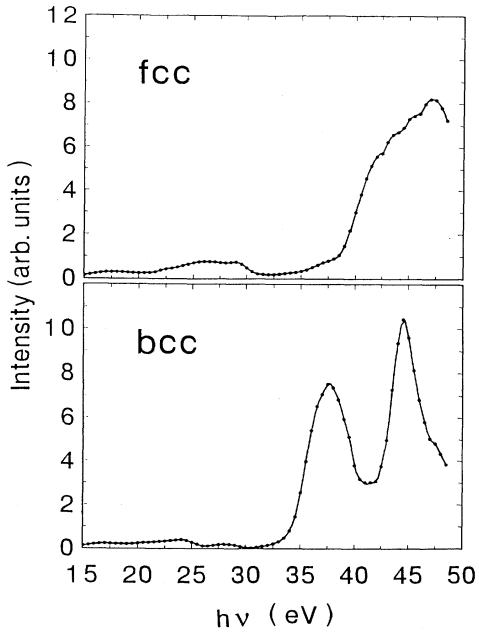

FIG. 18. Calculated peak heights in normal photoemission ($\alpha=45°$, $\Phi=0°$, *p*-polarized light) from the energetically lowest-lying full symmetric band for fcc (111) (above) and bcc (110) (below) silver shown as a function of photon energy $h\nu$.

to differentiate between bcc and fcc ordered Ag films. Therefore, we include an additional calculation which may help to differentiate between the two structures in future studies. In the following, we present calculated peak heights of two selected photoemission peaks in normal emission as a function of photon energy. Figure 18 shows calculated intensity (peak height) for the photoemission transition [$\Lambda_1 \rightarrow \Lambda_1$ for fcc (111) and $\Sigma_1 \rightarrow \Sigma_1$ for bcc (110)]. It is the emission from the energetically lowest-lying full symmetric band excited by light of energy $h\nu = 15-50$ eV. The intensity of photoemitted electrons exhibits a large broad peak for fcc structure. However, for bcc geometry the calculations predict two pronounced maxima divided by a minimum at about $h\nu \approx 41$ eV. This diverse behavior of intensity $I(h\nu)$ for fcc and bcc geometry is directly related to the band structure in the energy range of 35–50 eV. Bands of symmetry Σ_1 form a "gap" at $E_{\text{kin}} \approx 33-34$ eV. However, no similar structure is formed by the Λ_1 bands in this energy range. This feature should be well resolved in the normal photoemission spectrum. Unfortunately, to follow the abovementioned transition in experimental data is very difficult because of its very low intensity.

The characteristic minimum related to the "gap" in final states should be observable in intensities of other photoemission transitions unless a too large energetical dispersion of initial states does not remove it. Figure 19 shows the predicted effect of final states at $h\nu \approx 38$ eV on $I(h\nu)$ for the energetically highest-lying photoemission peak—in the theoretical model (see Fig. 1) the photoemission transitions excited from states at about 3.5 eV below E_F ($\Lambda_3 \rightarrow \Lambda_1$ for fcc and $\Sigma_1, \Sigma_3 \rightarrow \Sigma_1$ for the bcc structure). Note the substantially larger energy range of intensity decrease from the maximum at ≈ 32 eV for bcc structure in comparison with the fcc result.

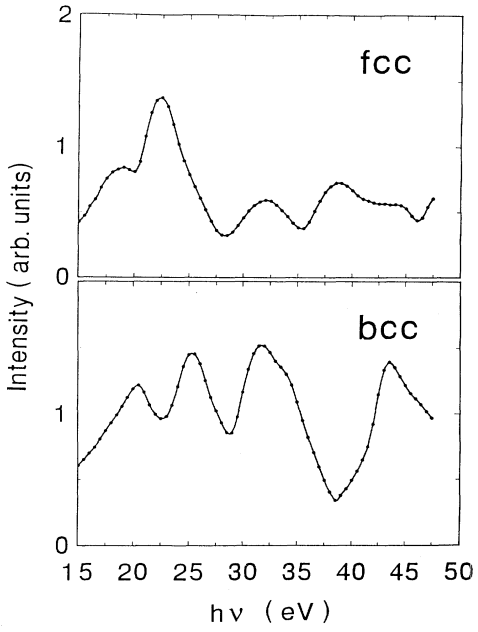

FIG. 19. Calculated peak heights of the normal photoemission structure at about −3.5 eV in the normal photoemission ($\alpha = 45°$, $\Phi = 90°$, p-polarized light) for fcc (111) (above) and bcc (110) (below) silver structures shown as a function of photon energy.

VI. CONCLUSION

Some evidence is given that Ag deposited onto cleaved InSb(110) surfaces at 10 K condenses for film thicknesses ≤ 30 ML in a bcc-like phase. For larger film thickness and for films with a thickness > 5 ML annealed to 300 K the known fcc Ag phase is found. The Ag 4d band spectra for a 60-ML film warmed to 300 K are better resolved than those for single-crystalline Ag(111) surfaces from the literature. We conclude that these films consist of large (111)-oriented Ag clusters which are, on the other hand, not large enough to produce a (111) LEED pattern. Our observation is in agreement with the general belief that photoemission is a more local probe than LEED.

We confirm the LEED observation of Aristov, Bolotin, and Grazhulis[18] that a bcc Ag(110) deposit grows on the InSb(110) surface at 10 K. In photoemission such a deposit of a mean thickness of 2.6 ML is not compatible with a fcc Ag band structure. Instead, it indicates a bcc-like band structure. Some indication for bcc Ag was also found for the 30-ML-thick film which was not annealed to 300 K. The difficulty of our measurements is due to the metastability of the bcc-like phase which prevents us from annealing these films in order to achieve a well-ordered film most appropriate for band-structure determination. For this reason, our analysis could also not differentiate between bcc and bcc tetragonal structures.

Nevertheless, our study strongly corroborates the earlier LEED study[18] and the total-energy calculations for Ag.[19,20] At 10 K, an appropriate substrate can impose a symmetry and atomic density of the Ag deposit which is better described by bcc than by fcc.

The above conclusions are based on the background of our calculation of the energy band structure for fcc and bcc Ag. From these calculations it becomes clear that the inclusion of SO interaction is necessary in order to achieve agreement between calculated and measured band structure.

Our investigation supports the idea of a bcc Ag phase under the influence of a reduced atomic density. Such a reduction in atomic density is experimentally realized here through epitactical growth of bcc Ag (110) on InSb(110).

In the outlook we have shown that for selected direct transitions in Ag we expect an even clearer differentiation between fcc and bcc Ag. This could be especially valuable in the case that one could realize a better ordered bcc phase.

Finally, we observe a weak quantum-well state. Its weakness may be explained through the missing order of the layer. The same is true for any lack of surface state at the fcc L gap or the bcc N gap as anticipated from the calculations.

ACKNOWLEDGMENTS

We want to thank P. Althainz and J. Schreiner for their help during the measurements and P. Geng for technical assistance. The support of the BESSY staff and especially of W. Braun, C. Jung, and C. Hellwig is appreciated. We are grateful to J. Kudrnovsky for providing scalar-relativistic calculations of silver band structures including spin-orbit coupling.

---

*Permanent address: Institute of Solid State Physics, Russian Academy of Sciences, Chernogolovka, Moscow district, 142432, Russian Federation.

†Present address: Sincrotrone Trieste, Padriciano 99, I-34012 Trieste, Italy.

‡Permanent address: Institute of Physics, Czechoslovak Academy of Sciences, Na Slovance 2, 180 40 Prague 8, Czechoslovakia.

[1]L. A. Bruce and H. Jaeger, Philos. Mag. **36**, 1331 (1977).

[2]Z. Q. Wang, S. H. Lu, Y. S. Li, F. Jona, and P. M. Marcus, Phys. Rev. B **35**, 9322 (1987).

[3]V. Yu. Aristov, I. L. Bolotin, and S. G. Gelakhova, Zh. Eksp. Teor. Fiz. **97**, 2005 (1990) [Sov. Phys. JETP **70**, 1134 (1990)].

[4]H. Li, D. Tian, J. Quinn, Y. S. Li, F. Jona, and P. M. Marcus, Phys. Rev. B **43**, 6342 (1991).

[5]B. Heinrich, A. S. Arrott, J. F. Cochran, C. Liu, and K. Myrtle, J. Vac. Sci. Technol. A **4**, 1374 (1986).

[6]Z. Q. Wang, Y. S. Li, F. Jona, and P. M. Marcus, Solid State Commun. **61**, 623 (1987).

[7]G. A. Prinz, Phys. Rev. Lett. **54**, 1051 (1985).

[8]J. G. Wright, Philos. Mag. **24**, 217 (1971).

[9]W. Kummerle and U. Gradmann, Solid State Commun. **24**, 33 (1971).

[10]W. Kuene, R. Holbauer, U. Gonzer, J. Lauer, and D. L. Williamson, J. Appl. Phys. **48**, 2976 (1977).

[11]P. A. Montano, Y. C. Lee, J. Marcano, and H. Min, in *Layered Structures and Epitaxy,* MRS Symposia Proceedings No. 56, edited by J. M. Gibson, G. C. Osbourn, and R. M. Tromp (Materials Research Society, Pittsburgh, 1986), p. 183.

[12]H. Li, S. C. Wu, D. Tian, J. Quinn, Y. S. Li, F. Jona, and P. M. Marcus, Phys. Rev. B **40**, 5841 (1989).

[13]D. Tian, S. C. Wu, F. Jona, and P. M. Marcus, Solid State Commun. **70**, 199 (1989).

[14]J. Quinn, Y. S. Li, H. Li, D. Tian, F. Jona, and P. M. Marcus, Phys. Rev. B **43**, 3959 (1991).

[15]I. A. Morrison, M. H. Kang, and E. J. Mele, Phys. Rev. B **39**, 1575 (1989).

[16]C. Chen, Phys. Rev. B **43**, 6347 (1991).

[17]F. Maca and J. Koukal, Surf. Sci. **260**, 323 (1992).

[18]V. Yu. Aristov, I. L. Bolotin, and V. A. Grazhulis, J. Vac. Sci. Technol. B **5**, 992 (1987).

[19]M. Said, F. Maca, K. Kambe, M. Scheffler, and N. E. Christensen, Phys. Rev. B **38**, 8505 (1988).

[20]F. Maca, K. Kambe, and M. Scheffler, Vacuum **41**, 538 (1990).

[21]H. Eckardt, L. Fritsche, and J. Noffke, J. Phys. F **14**, 97 (1984).

[22]V. Yu. Aristov, M. Bertolo, P. Althainz, and K. Jacobi, Surf. Sci. **281**, 74 (1993).

[23]V. L. Moruzzi, J. F. Janak, and A. R. Williams, *Calculated Electronic Properties of Metals* (Pergamon, New York, 1978).

[24]H. Wern, R. Courths, G. Leschik, and S. Hüfner, Z. Phys. B **60**, 293 (1985).

[25]O. K. Andersen and O. Jepsen, Phys. Rev. Lett. **53**, 2571 (1984); O. K. Andesen, Z. Pawlowska, and O. Jepsen, Phys. Rev. B **34**, 5253 (1986).

[26]Potential parameters including SO are taken from O.K. Andersen, O. Jepsen, and O. Glötzel, in *Highlights of Condensed Matter Theory,* edited by F. Bassani, F. Fumi, and P. M. Tosi (North-Holland, Amsterdam, 1985), p. 59.

[27]K. Jacobi, M. Scheffler, K. Kambe, and F. Forstmann, Solid State Commun. **22**, 17 (1977).

[28]M. Scheffler, K. Kambe, and F. Forstmann, Solid State Commun. **23**, 789 (1977).

[29]B. Frick and K. Jacobi, Surf. Sci. **178**, 907 (1986).

[30]D. E. Eastman, in *Techniques in Metals Research,* edited by E. Parsaglia (Interscience, New York, 1972), Vol. 6, p. 443.

[31]H. Höchst and I. Hernández-Calderón, Phys. Rev. B **30**, 4228 (1984).

[32]A. Förster, M. Tulke, and H. Lüth, J. Vac. Sci. Technol. B **5**, 1054 (1987).

[33]J. R. Chelikowsky and M. L. Cohen, Phys. Rev. B **14**, 556 (1976).

[34]C. Mailhiot, C. B. Duke, and D. J. Chadi, Phys. Rev. B **31**, 2213 (1985).

[35]M. A. Mueller, T. Miller, and T.-C. Chiang, Phys. Rev. B **41**, 5214 (1990).